THE JOURNAL OF BIOLOGICAL CHEMISTRY VOL. 283, NO. 27, pp. 18513–18521, July 4, 2008
Printed in the U.S.A.

# Plasma Membrane Cholesterol Content Affects Nitric Oxide Diffusion Dynamics and Signaling*

Received for publication, January 17, 2008, and in revised form, April 2, 2008 Published, JBC Papers in Press, April 29, 2008, DOI 10.1074/jbc.M800440200

**Shane Miersch[‡], Michael Graham Espey[§], Ruchi Chaube[‡], Arzu Akarca[‡], Rodney Tweten[¶], Sirinart Ananvoranich[‡], and Bulent Mutus[‡1]**

*From the [‡]Department of Chemistry and Biochemistry University of Windsor, Windsor Ontario N9B 3P4, Canada, the [¶]Department of Microbiology and Immunology, University of Oklahoma Health Sciences Center, Oklahoma City, Oklahoma 73104, and the [§]Molecular and Clinical Nutrition Section, NIDDK, National Institutes of Health, Bethesda, Maryland 20892-1372*

**Nitric oxide (NO) signaling is inextricably linked to both its physical and chemical properties. Due to its preferentially hydrophobic solubility, NO molecules tend to partition from the aqueous milieu into biological membranes. We hypothesized that plasma membrane ordering provided by cholesterol further couples the physics of NO diffusion with cellular signaling. Fluorescence lifetime quenching studies with pyrene liposome preparations showed that the presence of cholesterol decreased apparent diffusion coefficients of NO ~20–40%, depending on the phospholipid composition. Electrochemical measurements indicated that the diffusion rate of NO across artificial bilayer membranes were inversely related to cholesterol content. Sterol transport-defective Niemann-Pick type C1 (NPC1) fibroblasts exhibited increased plasma membrane cholesterol content but decreased activation of both intracellular soluble guanylyl cyclase and vasodilator-stimulated phosphoprotein (VASP) phosphorylation at Ser$^{239}$ induced by exogenous NO exposure relative to their normal human fibroblast (NHF) counterparts. Augmentation of plasma membrane cholesterol in NHF diminished production of both cGMP and VASP phosphorylation elicited by NO to NPC1-comparable levels. Conversely, decreasing membrane cholesterol in NPC1 resulted in the augmentation in both cGMP and VASP phosphorylation to a level similar to those observed in NHF. Increasing plasma membrane cholesterol contents in NHF, platelets, erythrocytes and tumor cells also resulted in an increased level of extracellular diaminofluorescein nitrosation following NO exposure. These findings suggest that the impact of cholesterol on membrane fluidity and microdomain structure contributes to the spatial heterogeneity of NO diffusion and signaling.**

As a small sized gaseous free radical, nitric oxide (NO)[2] presents unique challenges toward understanding the nature of its signaling in biological systems. Numerous levels of regulation at the level of nitric oxide synthase catalysis influence the rate of NO generation. Spatial localization of the biological signal is secondarily determined by a combination of the distinct physical and chemical properties of NO within the context of the microenvironment in which it was formed. The lifetime of NO molecules is governed chiefly by their relative abundance in relation to other radicals (1, 2), transition metal centers (3, 4), and oxygen ($O_2$) (5, 6). In addition to its very small size, the diffusional path of NO from the point of origin is affected by its preferentially hydrophobic solubility (7, 8), resulting in an enrichment of NO in biological membranes relative to the aqueous milieu. In the present work, the hypothesis that cells may utilize plasma membrane cholesterol to further orchestrate spatial heterogeneity in NO biological signaling activity was tested.

Cholesterol, a major lipid component of the plasma membrane in eukaryotic cells, plays an essential role in maintaining membrane fluidity and architecture (9–11). Cells tightly control the ratio of cholesterol and phospholipids in membranes to best suit their biological functions. Within the plasma membrane, cholesterol segregated with sphingolipids and selective proteins form distinct lipid raft complexes that act as ordered platforms for communicating signals into and out of cells (12). Dysregulation of cholesterol synthesis and transport acts as a contributing factor to pathophysiological changes (13–17), which are of particular importance in cardiovascular disease, chronic inflammation, and lipid disorders such as Niemann-Pick disease. The influence of cholesterol on NO diffusion was directly quantified in liposomal and artificial bilayer preparations. Soluble guanylyl cyclase (sGC) activation, VASP phosphorylation (Ser$^{239}$), and extracellular diaminofluorescein (DAF) nitrosation were used to investigate the effect of cellular plasma membrane cholesterol content on NO signaling dynamics. Taken together, these data show that plasma membrane cholesterol content modulates the level and type of NO signaling; pathological alterations in levels and distribution of

* This work was authored, in whole or in part, by National Institutes of Health staff. This work was supported by a National Suborbital and Educational Research Center (NSERC) Discovery Grant (to M. G. E.) and a Canadian Institutes of Health Research operating (bridging) grant (to B. M.). The costs of publication of this article were defrayed in part by the payment of page charges. This article must therefore be hereby marked "*advertisement*" in accordance with 18 U.S.C. Section 1734 solely to indicate this fact.

[1] To whom correspondence should be addressed: 401 Sunset Ave., Windsor, Ontario N9B 3P4, Canada. Fax: 519-973-7098; E-mail: mutusb@uwindsor.ca.

[2] The abbreviations used are: NO, nitric oxide; cGC, guanylate cyclase; DAF, diaminofluorescein; DEA/NO, 2-(*N*,*N*-diethylamino)-diazenolate-2-oxide diethylammonium salt; DPPC, dipalmitoylphosphatidyl choline; DMPC, dimyristoylphosphatidyl choline; DPTA, diethylenetriaminepentaacetic acid; BLM, bilayer lipid membrane; M$\beta$CD, methyl-$\beta$-cyclodextrin; Mn(III)-TMPyP, Mn(III)tetrakis(1-methyl-4-pyridyl) porphyrin pentachloride; NPC1, Niemann-Pick type C1; NHF, normal human fibroblast(s); PBS, phosphate-buffered saline; PFO-D4, perfringolysin-O domain 4; VASP, vasodilator-stimulated phosphoprotein; phospho-VASP, serine 239-phosphorylated VASP; CHAPS, 3-[(3-cholamidopropyl)dimethylammonio]-1-propanesulfonic acid; SV, Stern-Volmer.

cellular cholesterol may constitute a mechanism of errant NO signaling.

## EXPERIMENTAL PROCEDURES

Tris base, EDTA, phenylmethylsulfonyl fluoride, $N^G$-monomethyl-L-arginine, diaminofluorescein diacetate, dimyristoylphosphatidylcholine, dipalmitoylphosphatidylcholine, cholesterol, Dulbecco's modified Eagle's medium, diethylaminetriamine pentaacetic acid (DTPA), hemoglobin, sodium dithionite, malachite green, ammonium molybdate, and performic acid were obtained from Sigma. Alexa 532 succinimidyl ester and the Amplex Red cholesterol assay kit were obtained from Invitrogen. 1-Hexadecanoyl-2-(1-pyrenedecanoyl)-*sn*-glycero-3-phosphocholine was from Cayman Chemicals (Ann Arbor, MI). Mn(III)tetrakis(1-methyl-4-pyridyl) porphyrin pentachloride (Mn(III)TMPyP) was from Cedarlane Laboratories (Hornby, Canada). The cGMP enzyme immunoassay kit was from Amersham Biosciences. NO (gas), 10% with argon balance (BOC Gases, Mississauga, Canada), was purified by bubbling though 1 M KOH solution and used directly for experiments or dissolved in deoxygenated PBS with 500 $\mu$M DTPA and quantified spectrophotometrically by a hemoglobin assay as previously described (18). Normal human fibroblasts (HFF-1) and MCF-7 mammary epithelial cells (HTB-22) were obtained from ATCC (Manasass, VA), and NPC1 fibroblasts (GM17923) were from the Coriell Cell Repository (Camden, NJ). Cells were maintained in Dulbecco's minimal essential medium supplemented with 10% fetal calf serum and cultivated at 37 °C under an atmosphere of 5% $CO_2$. Erythrocytes and platelets were isolated from freshly drawn whole blood by differential centrifugation as indicated.

*NO Diffusion Measured by Quenching of Excited State Pyrene-labeled Membrane Lipids*—The interaction of excited state pyrene moieties with paramagnetic species, such as NO and $O_2$, are diffusion-controlled processes (19) and have previously been used to monitor the diffusion of nitric oxide in hydrophobic environments, allowing determination of apparent diffusion coefficients (20–22). We thus prepared liposomes of either dimyristoyl- or dipalmitoylphosphatidylcholine in the presence or absence of 33 mol % cholesterol doped with 1-hexadecanoyl-2-(1-pyrenedecanoyl)-*sn*-glycero-3-phosphocholine as previously described. Briefly, KOH-scrubbed nitric oxide from a 10% gas mixture (balance argon) was bubbled into oxygen-free liposome samples in sealed cuvettes equilibrated to 37 °C while monitoring fluorescence quenching ($\lambda_{ex}$ = 337 nm, $\lambda_{em}$ = 376 nm) in a Cary Eclipse fluorescence spectrometer (Cary Eclipse, Varian, Mississauga, Canada). 10-$\mu$l aliquots were removed with a gas-tight syringe, and NO was determined by an NO-specific electrode and comparison with a standard curve. Stern-Volmer plots were constructed by plotting the fractional quenching observed against the measured [NO] for not less than five replicate runs each with a coefficient of linearity >0.95. Quenching constants ($k_q$) were then determined from the slope ($k_q = k_{sv}/\tau$) using previously published fluorescence lifetimes ($\tau_o$) of 178 and 194 ns for DMPC and DMPC-cholesterol and 163 ns in DPPC and 178 ns in DPPC-cholesterol (23). Diffusion coefficients ($D$) were calculated from the Einstein-Smoluchowski equation ($k_q = 4\pi RDN$) (20), (where $R$ represents the sum of the molecular radii ($6 \times 10^8$ cm$^{-1}$) (19) and $N$ is Avogadro's number) and subsequently used to calculate membrane transit times using the equation $\langle x \rangle^2 = 2Dt$ (24).

*NO Diffusion in a BLM Chamber*—The BLM chamber was purchased from Eastern Scientific (Rockville, MD). The desired ratios of cholesterol/phospholipid were prepared in decane in a vial sealed with a septum and purged with $N_2$ (gas). A 5-$\mu$l aliquot of this solution was withdrawn and placed on the 1-mm hole in the Teflon divider in the BLM chamber. Both sides of the chamber were then filled with PBS at a rate of 500 $\mu$l/min. The entire BLM chamber was maintained at 37 °C, and both sides of the chamber were stirred with the aid of micro-stir bars. The formation of the lipid bilayer was monitored by the saturation of capacitance and by visual inspection. A constant amount of NO (gas) (ultrapure 1%, 99% argon), 200 $\mu$l/min, was metered out with a Matheson gas regulator (FM-1050) and introduced to one side of the chamber. The amount of NO (aq) diffusing through the BLM was measured with an NO electrode (WPI, Inc.) as a function of time and recorded digitally via Duo-18 software (WPI).

*Synthesis, Purification, and Alexa 532 Labeling of PFO-D4*—Plasmid pRT10 containing the perfringolysin O gene (*pfoA*) was used to construct the *pfoA* derivative D4 encoding the C-terminal region of the toxin. The DNA fragment containing the D4 ($Lys^{391}$–$Asn^{500}$)-encoding region was PCR-amplified using pRT10 plasmid as the template and ligated into the pTrcHisB expression vector, inserting it between the BamHI and KpNI restriction sites on the 3′-end of the sequence encoding the His tag site. The polymerase chain reaction primers used were as follows: forward primer, 5′-CCCGGATCCGTCTACAGAGTATTCTAAGG-3′; reverse primer, 5′-CCCGGTACCGGATTGTAAGTAATACTAGATCC-3′.

His-tagged PFO-D4 was isolated on a $Ni^{2+}$ affinity column after successive washes totaling 8 column volumes with 30 mM imidazole in 100 mM Tris buffer, pH 8.0. PFO-D4 was eluted with 100 mM imidazole in pH 8.0 100 mM Tris buffer and concentrated, and purity was demonstrated to be >95% by image analysis on a 15% SDS-polyacrylamide gel. Isolated PFO-D4 extensively dialyzed and labeled overnight with a 5-fold molar excess of Alexa 532 succinimidyl ester ($\epsilon$ = 81000 liters mol$^{-1}$ cm$^{-1}$) at 4 °C, separated from unreacted dye on a Sephadex-G25 column, and the extent of labeling was calculated as the molar ratio of dye to protein.

*Preparation of Cholesterol-loaded Cyclodextrin*—Cyclodextrin was charged with cholesterol as per previously described methods (25).

*Modulation of Cellular Plasma Membrane Cholesterol*—Cellular cholesterol was augmented by treatment with cholesterol-loaded methyl-$\beta$-cyclodextrin (M$\beta$CD) adduct. In brief, suspensions of $10^6$ trypsinized cells in PBS containing 500 $\mu$M DTPA were incubated with 100 $\mu$M adduct (determined on the basis of cholesterol by enzymatic assay) for 15 min with gentle nutation. Alternately, cellular cholesterol could be depleted using either apo-M$\beta$CD or cholesterol oxidase. Thus, $10^6$ cells in suspension were incubated with either 5 mM M$\beta$CD for 1 h or 2 units/ml cholesterol oxidase for 15 min at 37 °C with gentle rotation. Following cellular treatment, cholesterol-modulating agents were removed, and cells were used for experimentation.

*Imaging of Cellular Plasma Membrane Cholesterol with Alexa 532-labeled PFO-D4*—Cells on coverslips were fixed for 15 min at room temperature with 2% paraformaldehyde in HEPES buffer, washed three times, and stained with 400 nM Alexa 532-labeled PFO-D4 for 30 min with gentle shaking. Cells were washed again three times and imaged on an Axiovert epifluorescence microscope with 535 nm/550 nm excitation/emission under identical exposure conditions. Images were pseudocolored red using Northern Eclipse 6.0 imaging software, and the average intensity per unit of cell area was measured for 50–80 cells from not less than three independent slides of cells.

*Isolation and Characterization of NHF/NPC1 Plasma Membrane Lipids*—The cells of 3 T75 flasks at ~85% confluence were trypsinized and washed once with 100 mM Tris buffer, pH 7.4, and then once with 10 mM hypotonic Tris buffer, pH 7.4, containing 2 mM EDTA and 1 mg of phenylmethylsulfonyl fluoride. A 1-ml suspension was then homogenized by 50 strokes in a Dounce homogenizer. Mechanical disruption was verified by microscopic inspection, and the homogenate was spun at 190 × *g* for 10 min. Subsequent isolation of plasma membrane lipids was performed as previously described (16). Lipid suspension isolated in buffer was extracted twice with 200 μl of 1:1 MeOH/$CHCl_3$ and back-extracted once with 1 M NaCl, and the solvent was evaporated in a glass tube under a gentle stream of nitrogen.

*Western Analysis of PM Proteins*—10 μg of protein from each lipid suspension isolate was loaded into separate wells for resolution by SDS-PAGE. Proteins were then transferred to a polyvinylidene difluoride membrane and probed with primary antibodies to transferrin receptor, PDI, and LAMP1, followed by treatment with secondary antibodies conjugated to horseradish peroxidase. The bands were visualized with a chemiluminescent horseradish peroxidase substrate (Pierce).

*Phospholipid Analysis*—Lipid film was dissolved in 200 μl of $HClO_3$ and digested for 60 min at 180 °C. Aliquots of the acidified digest were mixed with malachite green and ammonium molybdate, and the absorbance was measured at 630 nm using previously published methods (26). Phosphorous concentration was interpolated from a standard curve, and phospholipid content/$10^6$ cells was estimated by the following conversion factor: [phospholipid] (μmol) = [phosphorous] (μmol) × 25.

*Cholesterol Analysis*—Lipid film was sonicated in 200 μl of CHAPS/Triton/sodium cholate buffer, and cholesterol was quantified using a cholesterol oxidase enzymatic assay (Invitrogen) and interpolation from a standard curve. In brief, solubilized cholesterol is oxidized by cholesterol oxidase to the cholest-4-en-3-one, producing hydrogen peroxide as a reaction by-product. Cholesterol oxidase-mediated production of $H_2O_2$ is coupled to the oxidation of 10-acetyl-3,7-dihydroxyphenoxazine to the highly fluorescent resorufin product by horseradish peroxidase. Cholesterol determination was performed according to the manufacturer's instructions to monitor resorufin formation in a 96-well plate at 37 °C with an excitation/emission couple of 545/595 nm on a PerkinElmer Life Sciences Victor 3 fluorescent plate reader.

*cGMP Production and VASP Phosphorylation as Measures of Intracellular NO Signaling*—Cells were cultivated to ~85% confluence and treated with 500 μM L-NMMA for 2 h to inhibit endogenous NO production. The cells were incubated a further 2 min with the SOD mimetic Mn(III)TMPyP (5 μM) and exposed to the NO donor DEA/NO (1 μM and 3 μM) and left undisturbed for 10 min in the incubator. Cells were trypsinized, collected, washed once with PBS containing 500 μM DTPA, and counted. After being adjusted for cell density (~$5 \times 10^5$ cells/ml), the cells were centrifuged and lysed with buffer containing phosphodiesterase and protease inhibitors. The lysates were then analyzed for either cGMP with an enzyme immunoassay kit (Amersham Biosciences) or VASP and phospho-VASP by Western immunoblotting with VASP and phospho-VASP ($Ser^{239}$) antibodies (Cell Signaling Technologies, Danvers, MA).

*Measurement of $NO_x$-mediated Extracellular Nitrosation by Cell-impermeant DAF*—NO uptake and metabolism to species capable of nitrosating DAF was also monitored by the reaction of extracellular DAF-2 with NO supplied by exogenous NO donor in the presence of intact cells. Cells are capable of acting as "NO sinks" and will take up a portion of NO from an extracellular donor, thus preventing its reaction with a $NO_x$-sensitive fluorophore, such as DAF-2. This approach has the additional benefit of circumventing potential intracellular interferences, which can contribute to artifactual DAF-2T signals (27–29). Adherent NHF and NPC1-deficient fibroblasts and MCF-7 cells were trypsinized, collected, and washed once with and suspended in PBS containing 500 μM DTPA. Human red blood cells and platelets were isolated from whole blood by differential centrifugation and suspended in PBS containing 500 μM DTPA. Cells were suspended to a final concentration of 10 μM DAF-2 in a fluorescent microplate, and counts were optimized to consume ~50% of delivered NO upon the addition of 250 nM DEA/NO. Membrane cholesterol was then augmented or depleted as indicated above. Cell viability following treatment was measured by a trypan blue exclusion assay to be greater than 90% in all cases. Excess cholesterol adduct, cyclodextrin, or enzyme was removed, and cells were suspended in a 10 μM DAF solution in PBS containing 0.5 mM DTPA and then treated with the 250 nM DEA/NO for monitoring of evolved fluorescence over time in the wells of a 96-well microplate with shaking at 37 °C using an excitation/emission couple of 485/515 nm, unless otherwise indicated.

## RESULTS

*Cholesterol Attenuates Rates of NO-induced Pyrene Quenching in Liposomes*—The interaction between excited state pyrene moieties and paramagnetic species, such as NO and $O_2$, are diffusion-controlled processes (19) and have previously been used to determine apparent diffusion coefficients of NO in hydrophobic environments (20–22). Preparations of pyrene fluorochrome encapsulated with either dipalmitoylphosphatidyl choline (DPPC) and dimyristoylphosphatidyl choline (DMPC) liposomes were exposed to NO gas while sealed in cuvettes under anaerobic conditions. NO diffusion into the liposome was represented by fluorescence quenching of excited state pyrene molecules. These data were expressed as a Stern-Volmer (SV) relationship where the fractional quenching ($I_o/I$) obtained from fluorescence monitoring was plotted against the measured concentration of NO (Fig. 1, *A* and *B*). The addition

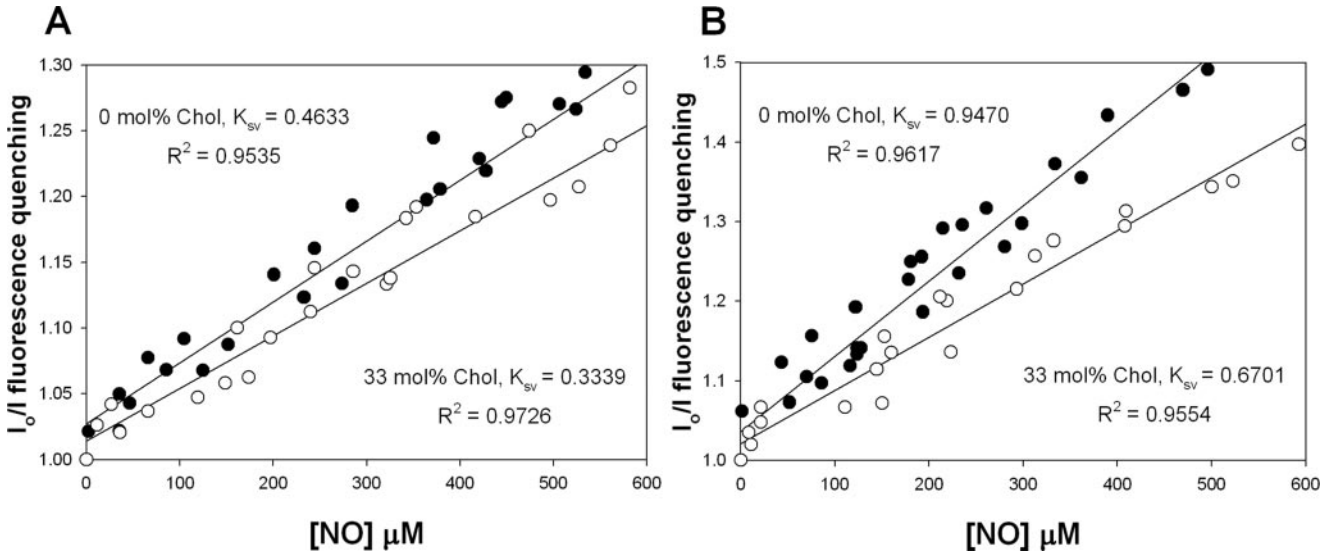


FIGURE 1. **Quenching of pyrene phospholipids in liposomes.** Stern-Volmer plots were obtained for deoxygenated suspensions of both DPPC (*A*) and DMPC (*B*) liposomes doped with 0.01 mol % 1-hexadecanoyl-2-(1-pyrenedecanoyl)-*sn*-glycero-3-phosphocholine in the presence (*filled squares*) and absence (*hollow squares*) of 33 mol % cholesterol containing 1.35 μmol of total lipid. Experiments were conducted at 37 °C in PBS with 500 μM DTPA and illustrate the fractional quenching ($I_o/I$) of the excited state pyrene moiety at various [NO] in the presence and absence of cholesterol.

of cholesterol (33 mol %) to either DPPC or DMPC liposomes resulted in a 28 and 29% decrease, respectively, in the slope ($K_{sv}$) of Stern-Volmer plot indicating a decrease in NO collisions with pyrene moieties within the lipid phase. The bimolecular quenching constant ($k_q$) for each liposome preparation was determined by dividing the $K_{sv}$ for each experiment by the previously published fluorescence lifetime ($\tau_o$) for each liposome mixture: $k_q = K_{sv}/\tau_o$. Apparent diffusion coefficients for NO were then estimated from the Einstein-Smoluchowski equation (24). These calculations indicated that the presence of cholesterol in DPPC and DMPC liposomes decreases the diffusion constants by ~24 and ~38%, respectively, suggesting a substantial influence of cholesterol over the diffusion of NO in a liposome environment (Table 1).

*Diffusion of NO across Bilayer Lipid Membranes Decreases as a Function of Increasing Cholesterol*—A NO-sensitive electrode was used to directly measure the relationship between cholesterol content and the rate of NO diffusion through an artificial bilayer membrane (BLM). A BLM composed of DPPC was prepared on a 1-mm hole in the gas-impermeable Teflon divider between two chambers containing phosphate-buffered saline (pH 7, 37 °C, stirring). The steady-state electrochemical signal recorded after the introduction of NO (1%, 200 μl/min) into the chamber opposing the electrode gave a trans-BLM membrane diffusion rate $V_{NO}$ of 0.0115 ± 0.00185 nmol of NO/min (Fig. 2). Under otherwise identical conditions, trans-BLM $V_{NO}$ decreased nonlinearly with increasing concentrations of cholesterol to 50% of the maximum $V_{NO}$ at ~17 mol % bilayer cholesterol content. The absence of linearity may be attributed to inhomogeneities in membrane structure induced by cholesterol rather than the effects of bulk cholesterol in the membrane. Taken together, these experiments provided readily quantifiable data showing that NO transit through membranes decreased as a function of cholesterol content.

*Niemann-Pick C1, Normal Human Fibroblasts, and Methyl-β-cyclodextrin Depletion/Repletion as a Model System for Altering Cellular Cholesterol Plasma Membrane Content*—NPC1 fibroblasts have been shown to exhibit a marked increase in plasma membrane cholesterol content (16) and decreased membrane fluidity relative to normal human fibroblasts (16, 17). Consistent with these reports, plasma membranes isolated from NPC1 fibroblasts were found to contain ~2-fold higher total cholesterol content relative to NHF, whereas a similar level of resident proteins (data not shown) and phospholipid content was present in both cell types (Fig. 3*A*). Microscopic visualization of cells labeled with perfringolysin domain 4 (PFO-D4)-specific probes that bind to cholesterol-enriched lipid raft microdomains (30) revealed two distinctive pheno-

**TABLE 1**
**Effect of cholesterol on the measured diffusion coefficients and resultant membrane transit times**

| | $k_q$ | $D$ (quencher) | Transit time |
|---|---|---|---|
| | $M^{-1}\,s^{-1}$ | $cm^2\,s^{-1}$ | μs |
| DPPC | $3.07 \times 10^9$ | $6.76 \times 10^{-6}$ | 1.48 |
| DPPC + 30% cholesterol | $2.25 \times 10^9$ | $4.95 \times 10^{-6}$ | 2.02 |
| DMPC | $5.06 \times 10^9$ | $1.11 \times 10^{-5}$ | 0.89 |
| DMPC + 30% cholesterol | $3.61 \times 10^9$ | $7.95 \times 10^{-6}$ | 1.25 |

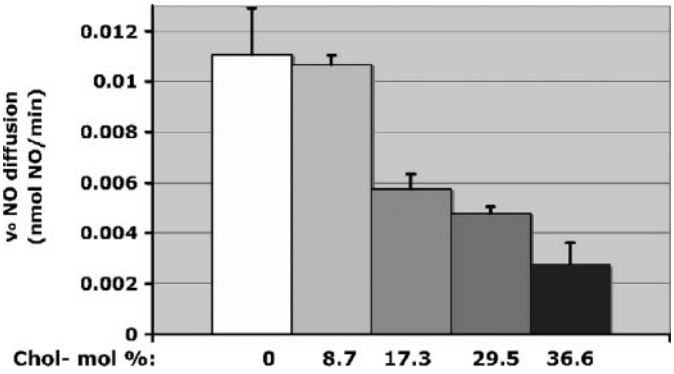


FIGURE 2. **Cholesterol-dependent NO diffusion through an artificial bilayer.** Rates of NO diffusion across the BLM as a function of BLM-cholesterol composition (mol %) ($n$ = 12 for each [cholesterol]).

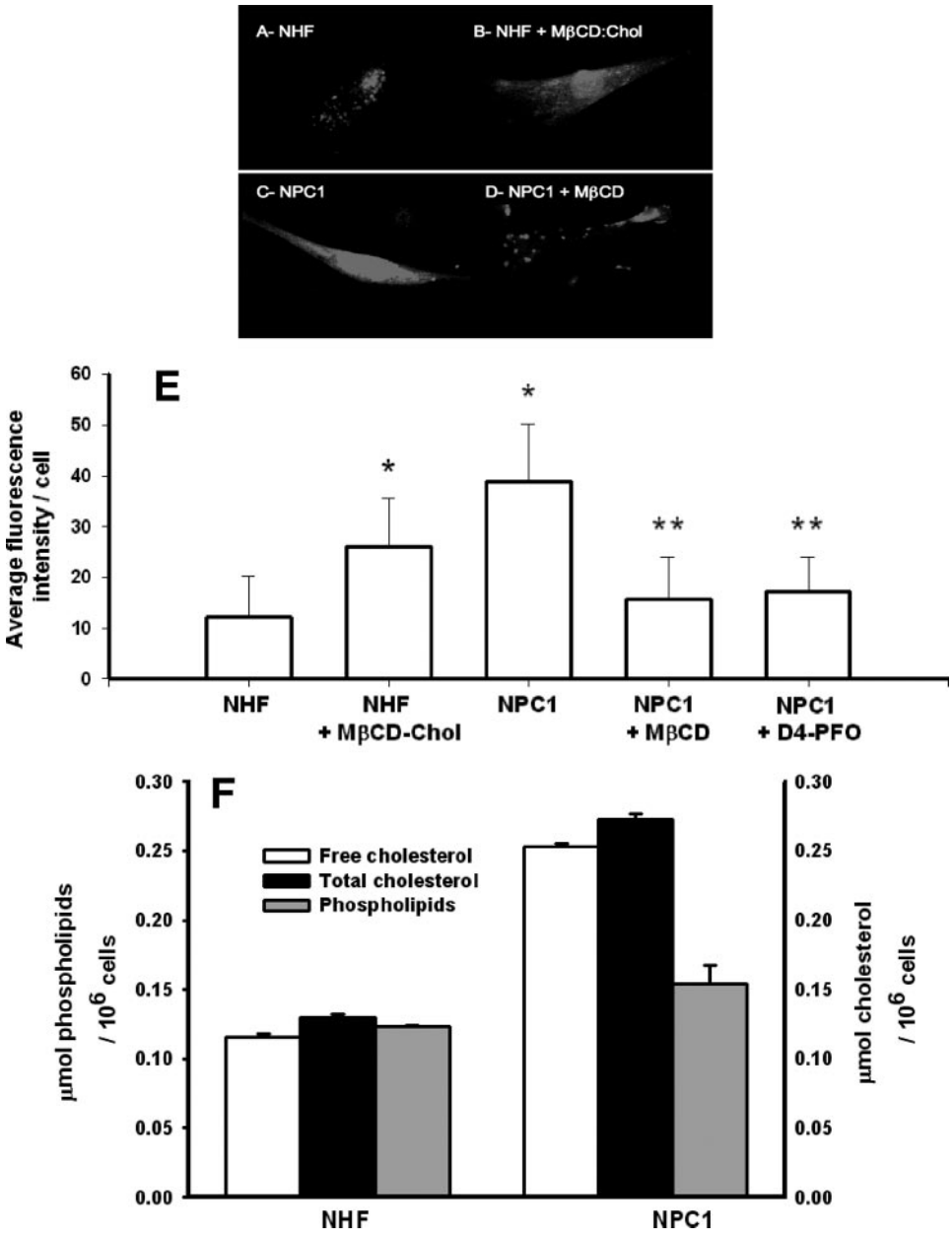


FIGURE 3. **PM cholesterol of NHF *versus* NPC1 fibroblasts by fluorescence imaging of D4 labeling and analysis of lipid isolates.** Fixed normal (*A*) and NPC1-deficient fibroblasts (*C*) stained with 400 nM Alexa 532-labeled D4 and imaged under identical exposure conditions exhibited cholesterol-dependent fluorescence. Normal human fibroblasts repeatedly stained less intensely than their NPC1-deficient counterpart. Importantly, treatment of NHF with 100 $\mu$M cholesterol-loaded M$\beta$CD was associated with an increase in cellular staining (*B*) and staining observed in NPC1-deficient cells could be largely abrogated by treatment with 10 mM M$\beta$CD prior to fixation (*D*). Data taken from 3–5 independently stained cell populations are summarized numerically from average intensities per cell for at least 50 cells (*E*). *Error bars*, S.D. *, $p < 0.005$ compared with NHF; **, $p < 0.001$ compared with NPC1; two-tailed *t* test. Cholesterol and phospholipid levels were determined from plasma membrane isolates obtained by sucrose gradient ultracentrifugation and are representative of two separate experiments with *error bars* showing S.D. (*F*).

typic patterns (Fig. 3, *B–E*). In contrast to the punctate staining of NHF, NPC1 fibroblasts exhibited a uniform distribution across the surface of the plasma membrane. In agreement with the isolated plasma membrane data, average intensity of PFO-D4 labeling per cell was 3.7-fold greater on NPC1 fibroblasts relative to NHF (Fig. 3*F*).

M$\beta$CD is a water-soluble cyclic oligosaccharide that either accepts or transfers a cholesterol molecule through interaction with the plasma membrane (23, 25). The capability to reverse the cholesterol phenotype of both NHF and NPC1 fibroblasts with M$\beta$CD was assessed by PFO-D4 labeling. Fig. 3, *C* and *F*, shows PFO-D4 labeling on NHF exposed to M$\beta$CD-cholesterol (100 $\mu$M, 1 h, 37 °C) increased in uniformity and intensity. NHF fractionation analysis revealed that M$\beta$CD-cholesterol resulted in a 4.25 ± 0.25-fold increase in plasma membrane cholesterol. The converse was evident with NPC1 fibroblasts M$\beta$CD alone, resulting in a 2.7-fold decrease in PFO-D4 staining intensity (Fig. 3, *D* and *F*).

*Cellular Plasma Membrane Cholesterol Content Shifts the Threshold for NO Activation of Cytoplasmic Soluble Guanylyl Cyclase and the Downstream cGMP-dependent Phosphorylation of VASP*—The NHF and NPC1 fibroblast model system was used to test the hypothesis that cholesterol levels in cellular plasma membranes affect NO signaling of intracellular targets. Activation of cytoplasmic sGC was utilized as a sensitive biosensor for changes in the level of extracellular NO diffusion through the plasma membrane. The contribution from endogenous NOS activity was negated by the presence of the NOS inhibitor $N^G$-monomethyl-L-arginine (500 $\mu$M). The levels of cGMP that accumulated in response to exogenous 1 and 3 $\mu$M DEA/NO exposures were 64% lower (*, $p < 0.001$; two-tailed *t* test) and 52% lower (*, $p < 0.001$; two-tailed *t* test), respectively, in NPC1 fibroblasts in comparison with that observed in an equivalent number of NHF (Fig. 4). When NHF were treated with M$\beta$CD-cholesterol to augment plasma membrane cholesterol to NPC1-equivalent levels, production of cGMP elicited by subsequent DEA/NO exposure was similar to NPC1 fibroblast responses (Fig. 4, *white to gray bars*). M$\beta$CD-cholesterol treatment decreased NHF cGMP levels 72% (**, $p < 0.001$; two-tailed *t* test) and 81% (**, $p < 0.001$; two-tailed *t* test) following either 1 or 3 $\mu$M DEA/NO exposure, respectively. In the reverse experiment, decreasing the plasma membrane in NPC1 by M$\beta$CD treatment increased cGMP production by 2.9-fold (***, $p < 0.001$; two-tailed *t* test) and 2.3-fold (***, $p < 0.001$; two-tailed *t* test) in response to 1 and 3 $\mu$M DEA/NO, respectively. In

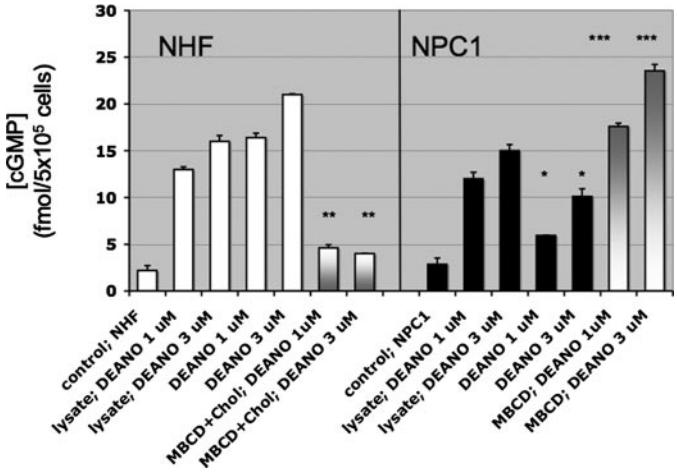


FIGURE 4. **Differential cGMP response of NHF and NPC1 fibroblasts to exogenous NO.** Cyclic guanosine monophosphate was measured by an enzyme immunoassay following stimulation of NHF (*white bars*) and NPC1-deficient fibroblasts (*black bars*) with the NO donor DEA/NO (1 and 3 $\mu$M). Shown is a comparison of [cGMP] in NPC1 fibroblasts with that observed in an equivalent number of NHF (*, $p < 0.001$; two-tailed *t* test); $n = 3$. Also shown is a comparison of [cGMP] in M$\beta$CD-cholesterol-treated NHF with NHF (*white to gray bars*; **, $p < 0.001$; two-tailed *t* test) and a comparison of [cGMP] in M$\beta$CD-treated NPC1 with NPC1 (*gray to white bars*; ***, $p < 0.001$; two-tailed *t* test); $n = 3$. In addition, [cGMP] levels in response to DEA/NO (1 and 3 $\mu$M) were compared in cell lysates of equal numbers of NHF and NPC1. *Error bars*, S.D.

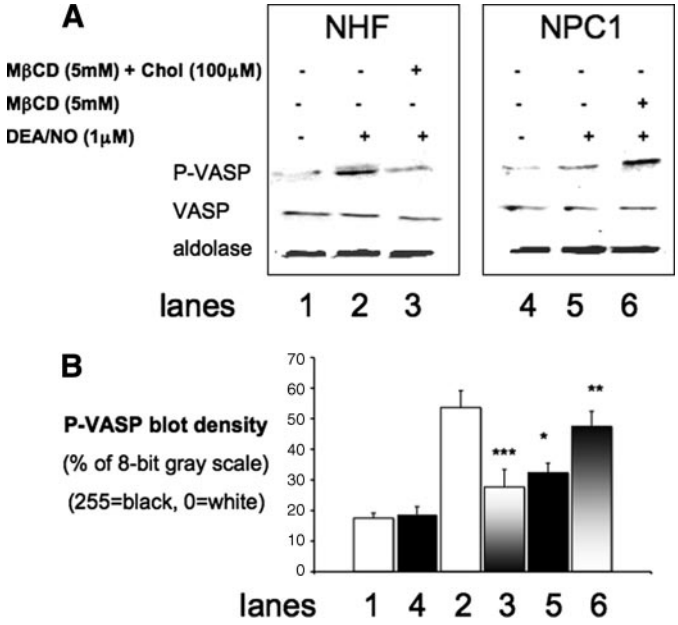


FIGURE 5. **Differential VASP Ser$^{239}$ phosphorylation response of NHF and NPC1 fibroblasts to exogenous NO.** *A*, the amount of VASP and phospho-Ser$^{239}$ VASP was estimated from Western immunoblots using equivalent numbers of NHF (*lanes 1–3*) and NPC1-deficient fibroblasts (*lanes 4–6*) probed with antibodies for phospho-VASP (*P-VASP*), VASP, and aldolase (loading control) in separate blots, subsequent to the exposure of the cells to DEA/NO (1 $\mu$M) (*lanes 2*, *3*, *5*, and *6*), NHF pretreated with M$\beta$CD-cholesterol (*lane 3*), or NPC1 pretreated with M$\beta$CD (*lane 6*). *B*, density plots of P-VASP data from Fig. 5*A*. Comparison of phospho-VASP in NPC1 fibroblasts with that observed in an equivalent number of NHF (*, $p < 0.033$; two-tailed *t* test); $n = 2$. Shown is a comparison of phospho-VASP in M$\beta$CD-treated NPC1 with NPC1 (*gray to white bars*; **, $p = 0.087$; two-tailed *t* test); $n = 2$. Also shown is a comparison of phospho-VASP in M$\beta$CD-cholesterol-treated NHF with NHF (*white to gray bars*; ***, $p = 0.0034$; 2-tailed *t* test); $n = 2$. Band density was estimated with ImageJ (1.39t) software. *Error bars*, S.D.

contrast, when the plasma membrane was ruptured by cellular lysis immediately prior to DEA/NO exposure, NPC1 produced 91% (1 $\mu$M DEA/NO) and 93% (3 $\mu$M DEA/NO) of the cGMP produced by NHF (Fig. 4). These data support the hypothesis that plasma membrane cholesterol levels can modulate the degree of cytoplasmic sGC activation by NO.

These data were extended to test whether variations in plasma membrane cholesterol affected downstream cGMP-mediated signaling. VASP is an actin-binding regulatory protein that is a substrate for both cGMP-protein kinase (at Ser$^{239}$) and cAMP-protein kinase (at Ser$^{157}$) (26–34). Consistent with cGMP data (Fig. 4), VASP Ser$^{239}$-phosphorylation in NPC1 cells exposed to DEA/NO (1 $\mu$M) was 40% less (*, $p = 0.033$, two-tailed *t* test) than levels observed in an equal number of identically treated NHF cells. Depletion of plasma membrane cholesterol from NPC1 cells with M$\beta$CD resulted in a proportionate increase in VASP Ser$^{239}$-phosphorylation (38%; **, $p = 0.087$, two-tailed *t* test) following NO exposure. Conversely, augmentation of plasma membrane cholesterol in NHF with M$\beta$CD-cholesterol resulted in the attenuation VASP phosphorylation by 50% ($p = 0.0034$, two-tailed *t* test) (Fig. 5, *A* and *B*). These results clearly demonstrate that plasma membrane cholesterol content can influence NO engagement with intracellular targets, such as sGC, thereby modulating downstream signaling through cGMP-protein kinase and VASP phosphorylation.

*Plasma Membrane Cholesterol Can Influence Formation of Extracellular Nitrosating Species*—An inverse relationship between plasma membrane cholesterol concentration and intracellular NO penetration was evident. We predicted that relatively higher levels of membrane cholesterol would result in an increased abundance of NO in the extracellular medium, thereby enhancing formation of the nitrosating species $N_2O_3$ through the autooxidation of NO. To test this hypothesis, cell suspensions were exposed to NO in the presence of extracellular 4,5-diaminofluorescein (31), and the formation of nitrosated fluorescent DAF-triazole product was monitored. The formation of DAF-triazole following the addition of exogenous NO (250 nM DEA/NO) to buffer alone or in the presence of either NHF or NPC1 fibroblasts is shown in Fig. 6*A*. These data indicated a higher level of extracellular DAF nitrosation elicited by NO autooxidation in the presence of NPC1 fibroblasts compared with NHF. DAF nitrosation was modestly increased 12.9 ± 7.1% ($p < 0.05$) when NHF cells were augmented with M$\beta$CD-cholesterol and washed prior to NO exposure (Fig. 6*B*). Similar enhancement of extracellular DAF nitrosation was observed with M$\beta$CD-cholesterol-treated platelets relative to corresponding untreated control cells during NO exposure (+28.0 ± 7.7%; $p < 0.001$). In the converse experiment, depletion of NPC1 plasma membrane cholesterol (−33.2 ± 1.4%) by incubation in cholesterol oxidase (0.2 units/ml, 37 °C, 15 min) followed by washing and suspension in DAF-containing buffer resulted in a 25 ± 14.2% decrease in DAF-triazole yield following NO exposure ($p < 0.05$ *versus* noncholesterol oxidase-treated NPC1).

Subtle changes in the dynamics between NO and superoxide can modulate the character of oxidative and nitrosative reaction pathways (32). Control experiments were performed to test whether M$\beta$CD-cholesterol treatment was influencing

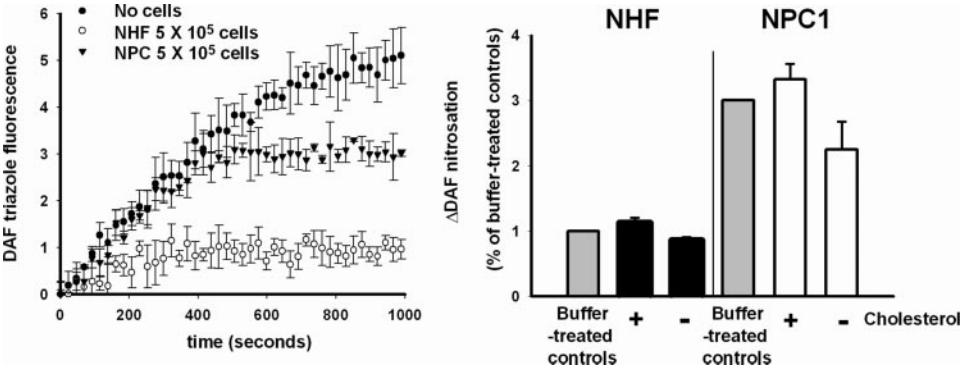


FIGURE 6. **DAF nitrosation in the presence of NHF *versus* NPC1 fibroblasts; effects of plasma membrane cholesterol modulation.** Cell suspensions containing $5 \times 10^5$ cells/ml with 10 $\mu$M DAF were treated with 250 nM DEA/NO in quadruplicate in a microwell plate, and the evolved fluorescence was intermittently monitored with shaking over the course of DEA/NO decomposition at 37 °C. Shown are representative traces from $n = 3$ experiments with *errors bars* calculated as the S.E. of $n = 4$ replicate samples and $p < 0.001$; two-tailed *t* test comparing the extent of nitrosation in the presence of NPC1 *versus* normal human fibroblasts (*A*). Shown are the collected results from experiments in which the membrane cholesterol was either enhanced (with 100 $\mu$M M$\beta$CD-cholesterol) or depleted (with 0.2 units/ml cholesterol oxidase) in both NHF (*black bars*) and NPC1-deficient cells (*white bars*). Shown are the collected results of maximum evolved fluorescence following complete decay of NO donor from $n = 3$ experiments, with *error bars* calculated as the S.D. of $n = 12$ samples. *, $p < 0.05$ *versus* buffer-treated controls (*gray bars*); two-tailed *t* test. **, $p > 0.05$ in the case of cholesterol-enhanced NPC1 cells; two-tailed *t* test (*B*).

DAF-triazole yield by altering cellular superoxide formation. Inclusion of either the enzyme superoxide dismutase (1 milliunit/ml) or porphyrin mimetic Mn(III)TMPyP (5 $\mu$M) did not significantly alter the enhanced nitrosation profiles for DAF in the buffer solutions in the presence of M$\beta$CD-cholesterol-treated cells relative to their untreated counterparts. Collectively, these data support the hypothesis that increased plasma membrane cholesterol levels correspondingly decrease NO entry into the cell, favoring a greater level of NO autooxidation and nitrosation of DAF present in the extracellular medium.

Data from liposome and artificial BLM experiments showed that increased cholesterol impedes diffusion of NO through lipid membranes (Figs. 1 and 2). A model system using NHF and cholesterol-enriched NPC1 fibroblasts was developed to examine whether plasma membrane cholesterol exerts influence on NO signaling in intact cells (Figs. 3–6). Comparative changes in NO signaling could be partially reversed in NHF or NPC1 fibroblasts by either increasing or decreasing respective membrane cholesterol levels.

## DISCUSSION

The aim of this study was to investigate whether plasma membrane cholesterol levels can modulate NO diffusion and cellular signaling. NO is generally held to traverse the plasma membrane freely (33) and would thus exhibit an identical ability to interact with cytoplasmic targets, such as sGC, regardless of membrane cholesterol content. However, results from our experiments with liposomal membranes doped with NO-reactive pyrene molecules revealed that NO diffusion rates were inversely related to cholesterol content (Fig. 1). An ~30% decrease in the NO diffusion coefficient was observed with DMPC liposomes bearing 30% cholesterol in comparison with liposome composed of phospholipid alone, which mirrors previously obtained results regarding the net flux of $O_2$ (34). Using planar bilayers, as little as 17 mol % cholesterol was required to decrease the transbilayer diffusion rate of NO 50%, whereas increasing the cholesterol fraction to 37 mol % resulted in a 75% decrease in diffusion rates (Fig. 2).

The Fick-Einstein theory of diffusion relates the size of a molecule to its diffusion. Due to the very small molecular radius of NO in comparison with most molecules, NO is predicted to move without hindrance between membrane moieties (35). Changes in the physical chemistry of membranes exerted by cholesterol have been theorized to occur in part through thermodynamic condensation of cholesterol with phospholipid acyl chains (36). Formation of these short range ordered complexes manifests a change in membrane fluidity, leading to a more tightly packed bilayer. Development dynamic spatial heterogeneities in the membrane milieu may account for results showing lower diffusivity of NO in relation to increased cholesterol (Figs. 1 and 2). Quantitative evidence from our synthetic systems presented herein supports the view that NO diffusion was sensitive to changes in local structural conformability and membrane viscosity imposed by increasing the molar fraction of cholesterol.

Data from synthetic liposome and BLM experiments raised the possibility that cholesterol levels in cellular membranes may have a significant impact on NO reactivity and signaling. Niemann-Pick C1 disease is an autosomal-recessive neurovisceral disorder characterized by defective endosomal cholesterol trafficking due to NPC1 gene mutation (37). Analysis of NPC1 fibroblasts revealed increased levels of plasma membrane cholesterol (2-fold) and cholesterol-enriched lipid rafts (3.7-fold) relative to NHF (Fig. 3). In support of the hypothesis, cGMP levels elicited in NPC1 fibroblasts exposed to NO were ~50% lower than that observed in their NHF counterparts (Fig. 4). Importantly, synthetic enrichment of NHF plasma membrane cholesterol (4-fold) by incubation with M$\beta$CD-cholesterol adducts resulted in a similar (~80%) decrease in cGMP elicited by NO compared with NHF with basal cholesterol (Fig. 4). Conversely, the depletion of plasma membrane cholesterol from NPC1 fibroblasts resulted in an ~2–3-fold increase in the amount of cGMP produced. Responses to NO by both NPC1 cells and NHF were within 93% of each other when plasma membranes were ruptured prior to NO exposure. These data are consistent with a diminished capability of exogenous NO molecules to permeate cellular plasma membranes as a function of increased cholesterol content, which was directly related to the activation of intracellular sGC.

Changes in membrane cholesterol were shown to influence targets downstream of sGC, such as the protein kinase-G substrate VASP, a mediator of cell motility, angiogenesis, vascular permeability, and platelet aggregation (27, 28–45). Fig. 5 shows that the level of VASP phosphorylation elicited by NO exposure could be manipulated by either augmentation or depletion of

plasma membrane cholesterol. These results suggest that hypercholesterolemia may globally infringe upon numerous cGMP-mediated signaling pathways.

The spatial heterogeneity that cholesterol adds to the plasma membrane may act to modulate sGC at several levels. Interestingly, calcium promotes sGC association with plasma membrane caveolae, specialized microdomains enriched with cholesterol (18, 26, 46). Due to the steep response curve of sGC to NO in the low nanomolar concentration range (28, 29), small decreases in NO transit through the membrane imposed by cholesterol could act to raise the threshold for sGC activation. In this light, Schmidt and co-workers (46) found that membrane-associated sGC exhibited an enhanced sensitivity to low levels of NO, whereas maximal sGC activity in response to high levels of NO was decreased in the membrane pool compared with the cytoplasmic fraction. In contrast with our findings, cholesterol depletion of endothelium-intact aortic rings by M$\beta$CD treatment disrupted sGC, protein kinase G, and caveolin-1 co-localization and impaired relaxation by sGC agonists (26). These studies and the present data together illustrate that plasma membrane cholesterol is dynamically linked to sGC signaling, with the direction and magnitude of its effect probably determined by configurations unique to cell types and activation states.

In addition to altering the threshold for sGC activation, the current study revealed that another consequence of plasma membrane cholesterol hindrance of NO ingress was to shift the chemical equilibrium for NO reactivity in the extracellular medium. A remarkable feature of NO formation is that the end effector nitrogen oxide species and biological outcomes can vary, dependent upon the context of the environment in which NOS catalysis occurs (32, 47). The findings showed that membrane cholesterol was inversely related to NO ingress. This suggested that increased plasma membrane cholesterol could shift the chemical equilibrium for NO reactivity in the extracellular medium. The rate of NO autooxidation is related to the square of NO concentration; therefore, an increased abundance of NO per unit of time favors formation of the nitrosating species $N_2O_3$ (6, 32, 48). NPC1 fibroblasts inherently laden with plasma membrane cholesterol (Fig. 3) displayed an increased nitrosation of extracellular DAF probe during NO exposure relative to NHF (Fig. 5). Moreover, converse results were obtained when plasma membrane cholesterol was either depleted or augmented in NPC1 and NHF cells, respectively. A 33% increase in extracellular DAF nitrosation was also observed with M$\beta$CD-cholesterol-loaded platelets during NO exposure relative to control platelets (data not shown). These experiments suggest that increased plasma membrane cholesterol content may influence the biological fate of NOS catalysis and signaling by shifting the balance from intracellular nitrosylation of heme protein targets, such as sGC, to formation of $N_2O_3$ and nitrosation of extracellular nucleophile moieties. In addition, hydrolysis of $N_2O_3$ to nitrite may decrease the overall aerobic bioactivity from NOS catalysis.

Cholesterol has been reported to act as a barrier to $O_2$ diffusion in synthetic membranes (50) as well as a determinant in $O_2$ gradients in cellular systems (51). However, cholesterol effects on $O_2$ were probably a negligible component in DAF results, because NO autooxidation is first order with respect to $O_2$, and experiments were conducted in an open system while stirring. The possibility that cholesterol manipulation in cells may result in generation of superoxide anion, which, depending on its ratio to NO, could account for the secondary formation of oxidants or nitrosating species (32), was taken into consideration. Differences in DAF-triazole yields were not observed with and without inclusion of the superoxide oxide dismutase enzyme or mimetic Mn(III)TmPyP in our cellular systems, ruling out a potential contribution of superoxide to the findings.

Hypercholesterolemia is a risk factor in a wide range of pathologies. Although data support the view that hypertension may be influenced by cholesterol dysregulation at the level of the caveolar architecture and its association endothelial NOS isoform, resulting in diminished NO bioavailability or altered NO signaling (52), the current work shows that cholesterol and NO also interact directly at the physical chemical level in the plasma membrane. It is important to note that the shift in the balance of NO signals in NPC1 fibroblasts from intracellular sGC nitrosylation toward extracellular nitrosation could readily be reversed solely by cholesterol depletion (Fig. 4). Whether cells utilize the local ordering effect of cholesterol to impart spatial control over physiological NO signaling at the membrane microdomain level remains a point for further investigation.

Recent studies by Freeman and co-workers (53–56) have demonstrated that membrane lipid raft density in cancer cells is intimately related to cell survival, since the depletion of raft cholesterol by statins increased the sensitivity of cancer cells to apoptosis. The proapoptotic effects were eliminated with replenishment of membrane cholesterol with M$\beta$CD-cholesterol (53–56). Although many of the cholesterol-sensitive signaling pathways are largely unknown, raft-resident protein kinase B$\alpha$ (Akt1) (57) complexed with androgen receptor (58) has been identified as a source of the antiapoptotic signaling in prostate cancer cells. Relationships between cholesterol rafts and statins are emerging in the etiology and treatment of neurodegenerative diseases (49, 59–61). Our new findings show that increased plasma membrane cholesterol content raises the threshold for exogenous NO to activate sGC and affect the downstream protein kinase G target VASP (Fig. 5).

Therefore, this study raises the possibility that the physical portioning of NO by membrane cholesterol rafts could be a contributing factor in the pathobiology of diseases beyond Neiman-Pick disorder, including cancer, neurondegeneration, and cardiovascular diseases. The present findings in both synthetic and live cell systems indicated that membrane cholesterol concentration influenced the physical diffusant, reactive chemistry, and cellular signaling qualities of NO.

## REFERENCES

1. Issner, R., Nauser, T., Bugnon, P., Lye, P. G., and Koppenol, W. H. (1997) *Chem. Res. Toxicol.* **10,** 1285–1292
2. Lima, E. S., Di Mascio, P., and Abdalla, D. S. (2003) *J. Lipid Res.* **44,** 1660–1666
3. Chiang, C. Y., and Darensbourg, M. Y. (2006) *J. Biol. Inorg. Chem.* **11,** 359–370
4. Mason, M. G., Nicholls, P., Wilson, M. T., and Cooper, C. E. (2006) *Proc. Natl. Acad. Sci. U. S. A.* **103,** 708–713

5. Caccia, S., Denisov, I., and Perrella, M. (1999) *Biophys. Chem.* **76,** 63–72
6. Lewis, R. S., and Deen, W. M. (1994) *Chem. Res. Toxicol.* **7,** 568–574
7. Wood, J., and Garthwaite, J. (1994) *Neuropharmacology* **33,** 1235–1244
8. Philippides, A., Husbands, P., and O'Shea, M. (2000) *J. Neurosci.* **20,** 1199–1207
9. Pucadyil, T. J., and Chattopadhyay, A. (2006) *Chem. Phys. Lipids* **143,** 11–21
10. Hao, M., Mukherjee, S., and Maxfield, F. R. (2001) *Proc. Natl. Acad. Sci. U. S. A.* **98,** 13072–13077
11. Rukmini, R., Rawat, S. S., Biswas, S. C., and Chattopadhyay, A. (2001) *Biophys. J.* **81,** 2122–2134
12. Simons, K., and Ikonen, E. (1997) *Nature* **387,** 569–572
13. Preston Mason, R., Tulenko, T. N., and Jacob, R. F. (2003) *Biochim. Biophys. Acta* **1610,** 198–207
14. Chen, M., Mason, R. P., and Tulenko, T. N. (1995) *Biochim. Biophys. Acta* **1272,** 101–112
15. Qin, C., Nagao, T., Grosheva, I., Maxfield, F. R., and Pierini, L. M. (2006) *Arterioscler. Thromb. Vasc. Biol.* **26,** 372–378
16. Vainio, S., Bykov, I., Hermansson, M., Jokitalo, E., Somerharju, P., and Ikonen, E. (2005) *Biochem. J.* **391,** 465–472
17. Koike, T., Ishida, G., Taniguchi, M., Higaki, K., Ayaki, Y., Saito, M., Sakakihara, Y., Iwamori, M., and Ohno, K. (1998) *Biochim. Biophys. Acta* **1406,** 327–335
18. Gomes, B., Savignac, M., Cabral, M. D., Paulet, P., Moreau, M., Leclerc, C., Feil, R., Hofmann, F., Guery, J. C., Dietrich, G., and Pelletier, L. (2006) *J. Biol. Chem.* **281,** 12421–12427
19. Birks, J. B. (1970) *The Photophysics of Aromatic Molecules*, Wiley Interscience, London
20. Denicola, A., Souza, J. M., Radi, R., and Lissi, E. (1996) *Arch Biochem. Biophys.* **328,** 208–212
21. Denicola, A., Batthyany, C., Lissi, E., Freeman, B. A., Rubbo, H., and Radi, R. (2002) *J. Biol. Chem.* **277,** 932–936
22. Möller, M., Botti, H., Batthyany, C., Rubbo, H., Radi, R., and Denicola, A. (2005) *J. Biol. Chem.* **280,** 8850–8854
23. Kilsdonk, E. P., Yancey, P. G., Stoudt, G. W., Bangerter, F. W., Johnson, W. J., Phillips, M. C., and Rothblat, G. H. (1995) *J. Biol. Chem.* **270,** 17250–17256
24. Einstein, A. (1905) *Annalen der Physik* **17,** 549–560
25. Christian, A. E., Haynes, M. P., Phillips, M. C., and Rothblat, G. H. (1997) *J. Lipid Res.* **38,** 2264–2272
26. Linder, A. E., McCluskey, L. P., Cole, K. R., III, Lanning, K. M., and Webb, R. C. (2005) *J. Pharmacol. Exp. Ther.* **314,** 9–15
27. Garcia Arguinzonis, M. I., Galler, A. B., Walter, U., Reinhard, M., and Simm, A. (2002) *J. Biol. Chem.* **277,** 45604–45610
28. Mo, E., Amin, H., Bianco, I. H., and Garthwaite, J. (2004) *J. Biol. Chem.* **279,** 26149–26158
29. Bellamy, T. C., and Garthwaite, J. (2002) *Mol. Cell Biochem.* **230,** 165–176
30. Ohno-Iwashita, Y., Shimada, Y., Waheed, A. A., Hayashi, M., Inomata, M., Nakamura, M., Maruya, M., and Iwashita, S. (2004) *Anaerobe* **10,** 125–134
31. Espey, M. G., Miranda, K. M., Thomas, D. D., and Wink, D. A. (2001) *J. Biol. Chem.* **276,** 30085–30091
32. Espey, M. G., Thomas, D. D., Miranda, K. M., and Wink, D. A. (2002) *Proc. Natl. Acad. Sci. U. S. A.* **99,** 11127–11132
33. Subczynski, W. K., Lomnicka, M., and Hyde, J. S. (1996) *Free Radic. Res.* **24,** 343–349
34. Fischkoff, S., and Vanderkooi, J. M. (1975) *J. Gen. Physiol.* **65,** 663–676
35. Möller, M. N., Li, Q., Lancaster, J. R., Jr., and Denicola, A. (2007) *IUBMB Life* **59,** 243–248
36. Radhakrishnan, A., and McConnell, H. (2005) *Proc. Natl. Acad. Sci. U. S. A.* **102,** 12662–12666
37. Zhang, M., Dwyer, N. K., Love, D. C., Cooney, A., Comly, M., Neufeld, E., Pentchev, P. G., Blanchette-Mackie, E. J., and Hanover, J. A. (2001) *Proc. Natl. Acad. Sci. U. S. A.* **98,** 4466–4471
38. Krause, M., Dent, E. W., Bear, J. E., Loureiro, J. J., and Gertler, F. B. (2003) *Annu. Rev. Cell Dev. Biol.* **19,** 541–564
39. Krause, M., Bear, J. E., Loureiro, J. J., and Gertler, F. B. (2002) *J. Cell Sci.* **115,** 4721–4726
40. Bear, J. E., Svitkina, T. M., Krause, M., Schafer, D. A., Loureiro, J. J., Strasser, G. A., Maly, I. V., Chaga, O. Y., Cooper, J. A., Borisy, G. G., and Gertler, F. B. (2002) *Cell* **109,** 509–521
41. Kwiatkowski, A. V., Gertler, F. B., and Loureiro, J. J. (2003) *Trends Cell Biol.* **13,** 386–392
42. Price, C. J., and Brindle, N. P. (2000) *Arterioscler. Thromb. Vasc. Biol.* **20,** 2051–2056
43. Massberg, S., Gruner, S., Konrad, I., Garcia Arguinzonis, M. I., Eigenthaler, M., Hemler, K., Kersting, J., Schulz, C., Muller, I., Besta, F., Nieswandt, B., Heinzmann, U., Walter, U., and Gawaz, M. (2004) *Blood* **103,** 136–142
44. Chen, L., Daum, G., Chitaley, K., Coats, S. A., Bowen-Pope, D. F., Eigenthaler, M., Thumati, N. R., Walter, U., and Clowes, A. W. (2004) *Arterioscler. Thromb. Vasc. Biol.* **24,** 1403–1408
45. Aszodi, A., Pfeifer, A., Ahmad, M., Glauner, M., Zhou, X. H., Ny, L., Andersson, K. E., Kehrel, B., Offermanns, S., and Fassler, R. (1999) *EMBO J.* **18,** 37–48
46. Zabel, U., Kleinschnitz, C., Oh, P., Nedvetsky, P., Smolenski, A., Muller, H., Kronich, P., Kugler, P., Walter, U., Schnitzer, J. E., and Schmidt, H. H. (2002) *Nat. Cell Biol.* **4,** 307–311
47. Espey, M. G., Miranda, K. M., Thomas, D. D., Xavier, S., Citrin, D., Vitek, M. P., and Wink, D. A. (2002) *Ann. N. Y. Acad. Sci.* **962,** 195–206
48. Wink, D. A., Darbyshire, J. F., Nims, R. W., Saavedra, J. E., and Ford, P. C. (1993) *Chem. Res. Toxicol.* **6,** 23–27
49. Reid, P. C., Urano, Y., Kodama, T., and Hamakubo, T. (2007) *J. Cell Mol. Med.* **11,** 383–392
50. Subczynski, W. K., Hyde, J. S., and Kusumi, A. (1989) *Proc. Natl. Acad. Sci. U. S. A.* **86,** 4474–4478
51. Khan, N., Shen, J., Chang, T. Y., Chang, C. C., Fung, P. C., Grinberg, O., Demidenko, E., and Swartz, H. (2003) *Biochemistry* **42,** 23–29
52. Sowa, G., Pypaert, M., and Sessa, W. C. (2001) *Proc. Natl. Acad. Sci. U. S. A.* **98,** 14072–14077
53. Freeman, M. R., and Solomon, K. R. (2004) *J. Cell. Biochem.* **91,** 54–69
54. Freeman, M. R., Cinar, B., and Lu, M. L. (2005) *Trends Endocrinol Metab.* **16,** 273–279
55. Zhuang, L., Kim, J., Adam, R. M., Solomon, K. R., and Freeman, M. R. (2005) *J. Clin. Invest.* **115,** 959–968
56. Freeman, M. R., Solomon, K. R., and Moyad, M. (2006) *J. Am. Med. Assoc.* **295,** 2720–2721
57. Adam, R. M., Mukhopadhyay, N. K., Kim, J., Di Vizio, D., Cinar, B., Boucher, K., Solomon, K. R., and Freeman, M. R. (2007) *Cancer Res.* **67,** 6238–6246
58. Cinar, B., Mukhopadhyay, N. K., Meng, G., and Freeman, M. R. (2007) *J. Biol. Chem.* **282,** 29584–29593
59. Ponce, J., de la Ossa, N. P., Hurtado, O., Millan, M., Arenillas, J. F., Dávalos, A., and Gasull, T. (2008) *Stroke* **39,** 1269–1275
60. Sagin, F. G., and Sozmen, E. Y. (2008) *Curr. Alzheimer Res.* **5,** 4–14
61. Ostrowski, S. M., Wilkinson, B. L., Golde, T. E., and Landreth, G. (2007) *J. Biol. Chem.* **282,** 26832–26844